(25 p.p.m. for 25 weeks). Thus, this analysis also revealed the induction of CYGB in fibrotic human livers (Figure 4b).

The scarcity of CYGB- and CRBP-1-positive cells in the fibrotic septum is convincingly shown in Figure 5. The distribution patterns of three myofibroblast biomarkers, α-SMA (Figure 5b, e, h, k, n), Thy-1 (Figure 5c, f, i, and l), and FBLN2 (Figure 5o), in the portal areas were nearly identical in fibrotic livers. The distribution of CYGB was mutually exclusive with the distribution of these three proteins (Figure 5a, d, g, j, and m).

The mutually exclusive localization patterns of these cell type-specific markers were further examined by double immunofluorescence staining (Figure 6). CYGB was expressed in cells close to the parenchymal area of F1 to F3 livers (Figure 6a, d, and g), and its expression did not overlap with that of α-SMA (Figure 6c, f, and i). However, in the F4 liver, cells near the extended fibrotic septum were double positive for CYGB and α-SMA, strongly suggesting that these cells were activated stellate cells. In the F3 liver, neither FBLN2 nor Thy-1 overlapped with CYGB (Figure 6m–r).

Taken together, these data reveal that CYGB and CRBP-1 are excellent markers of human stellate cells in both intact and fibrotic livers and that stellate cells become positive for α-SMA when activated. We hypothesize that cells positive for FBLN2 and Thy-1 are different from stellate cells and exhibit the phenotype of portal myofibroblasts that are α-SMA positive in intact human liver tissue.

Quantitative Analysis of the Contributions of Stellate Cells and Myofibroblasts to the Progression of Fibrosis

Of the 40 HCV-infected patients who underwent liver biopsy, the proportion of fibrotic area (as determined by Sirius red staining and immunostaining for α-SMA and Thy-1) was significantly correlated with the stage of liver fibrosis according to the new Inuyama classification. The Sirius red-positive area increased from 1.8% in F1 to 3.66%, 8.57%, and 16.8% in F2, F3, and F4, respectively (Figure 7a). Similarly, the α-SMA-positive area increased from 1.26% in F1 to 1.82%, 5.65%, and 8.31% in F2, F3, and F4, respectively (Figure 7b). The Thy-1-positive area increased from 1.13% in F1 to 2.13%, 5.43%, and 7.52% in F2, F3, and F4, respectively (Figure 7c). In contrast, the density of CYGB-positive cells (Figure 7d) and CRBP-1-positive cells (Figure 7e) was inversely correlated with the progression of liver fibrosis; the density of CYGB-positive cells was 17.9 ± 1.29, 19.7 ± 1.01, 16.2 ± 0.82, and 13.8 ± 1.06 cells/mm^2 in F1, F2, F3, and F4, respectively, and the density of CRBP-1-positive cells was 9.56 ± 1.24, 14.6 ± 0.77, 12.1 ± 0.83, and 9 ± 0.67 cells/mm^2 in F1, F2, F3, and F4, respectively.

CYGB Expression in Primary Mouse Stellate Cells

We determined above the *in vivo* expression profiles of cell type-specific biomarkers in stellate cells and myofibroblasts in intact and fibrotic human liver tissues. Next, we questioned whether these *in vivo* expression profiles could be reproduced in an *in vitro* system. We utilized primary cultures of mouse stellate cells rather than human stellate cells because human stellate cells in a normal quiescent stage are difficult to obtain for laboratory use. These cells were cultured for up to 7 days, during which changes in the expression levels of CYGB, α-SMA, and Thy-1 were immunohistochemically examined (Figure 8).

At 1 day of culture after isolation from the intact liver, mouse stellate cells adhered to plastic plates and exhibited round cell bodies with numerous lipid droplets similar to those observed in lipocytes (Figure 8aA). The cell bodies then began to gradually spread and flatten, and they successively increased in size and lost their lipid droplets, resulting in an activated myofibroblastic phenotype (Figure 8aB and C). Immunocytochemical analyses confirmed the consistent expression of CYGB until day 7 of culture (Figure 8aA–C). α-SMA was not observed at day 1 (Figure 8aD); however, it later appeared at days 4 and 7 (Figure 8aE and F). Double immunofluorescence analysis confirmed the presence of both CYGB and α-SMA in stellate cells at days 4 and 7 (Figure 8aH and J), although their intracellular localization patterns were different; Cygb was distributed diffusely in the cytoplasm, whereas α-SMA tended to accumulate at the periphery of the cells. Immunostaining for CRBP-1 and α-SMA yielded similar results, although CRBP-1 expression was decreased in 7-day-cultured stellate cells, presumably because of the loss of vitamin A in the cytoplasm (data not shown). Thy-1 was not observed throughout the culture period (Figure 8aM–O). The above-mentioned expression profiles of the marker proteins were confirmed by immunoblot analysis (Figure 8b). These results led us to hypothesize that the α-SMA-positive cells observed at later stages of culture were not myofibroblasts but rather activated stellate cells because they were Thy-1 negative.

DISCUSSION

Cytoglobin Is an Excellent Marker of Human Stellate Cells

CYGB was previously isolated from cultured rat hepatic stellate cells that have vitamin A storage ability in the quiescent state and function as liver-specific pericytes.[1]

Figure 5 Histological analyses of human liver fibrosis at different stages (F1 to F4) according to the new Inuyama classification. Immunohistochemistry for CYGB (**a**, **d**, **g**, **j**, **m**), α-SMA (**b**, **e**, **h**, **k**, **n**), Thy-1 (**c**, **f**, **i**, **l**), and FBLN2 (**o**). At each stage, CYGB (arrows) had limited expression in sinusoids, and the positive cells were deemed stellate cells. α-SMA was expressed in the vessel walls of the portal vein and artery, around bile ducts, and in the cells in Glisson's capsule. Some α-SMA-positive cells were also present in the parenchyma at stage F4 (**k**). Both Thy-1 and FBLN2 had limited expression in Glisson's capsule and the extended fibrotic septum in all stages of liver fibrosis. Bar, 50 μm. p, portal vein.

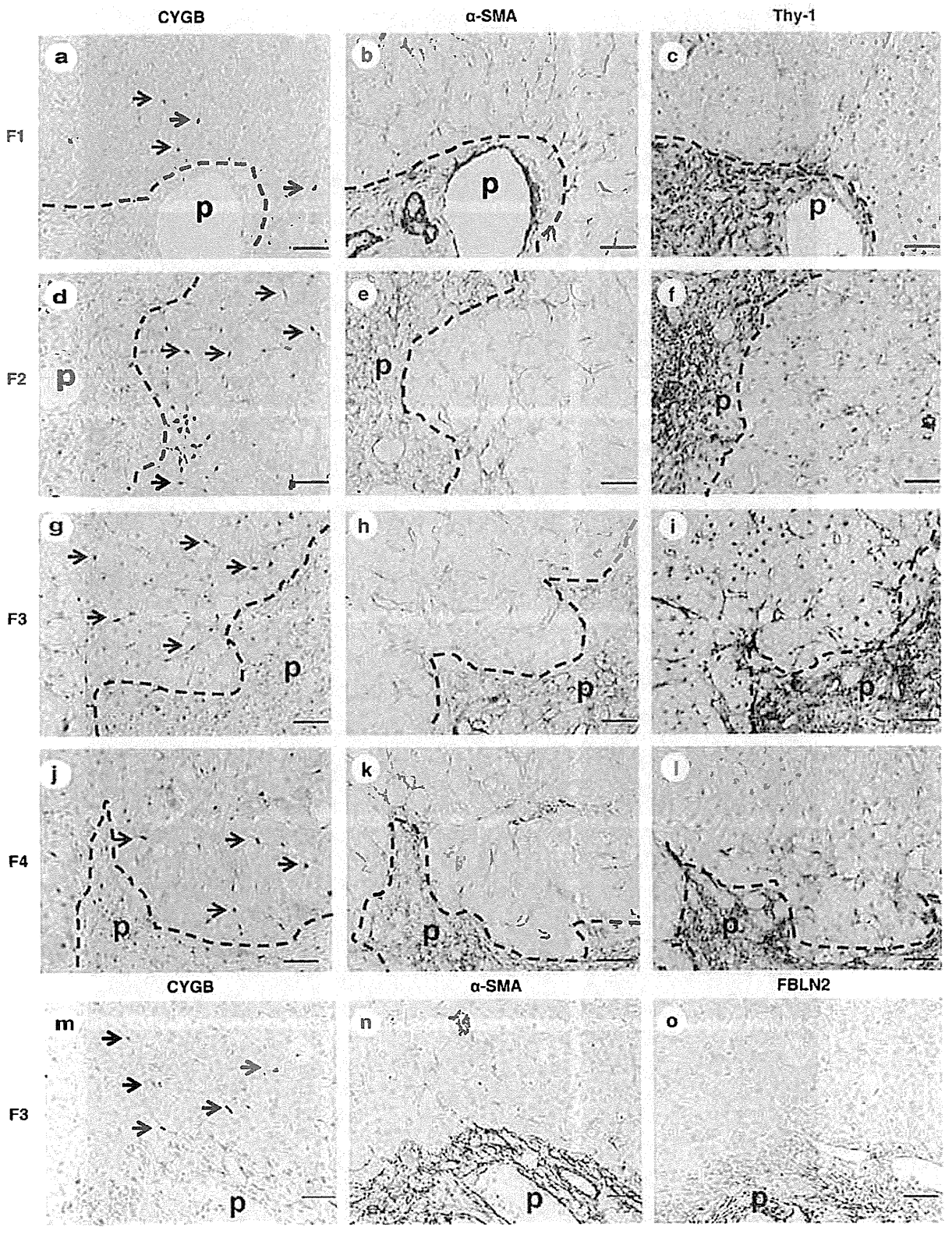
CYGB
α-SMA
Thy-1
F1
F2
F3
F4
F3
CYGB
α-SMA
FBLN2
a
b
c
d
e
f
g
h
i
j
k
l
m
n
o
p

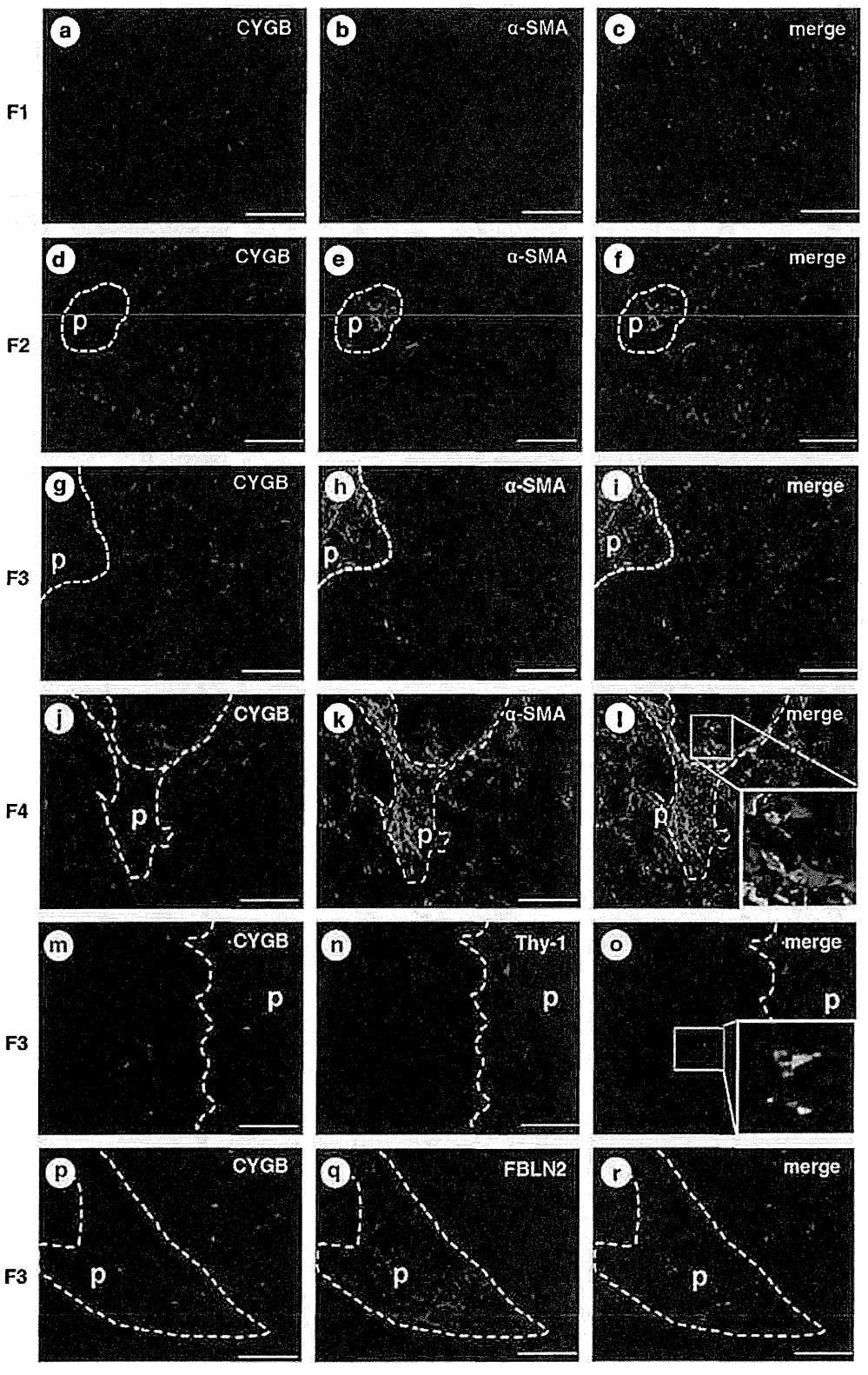
F1
a
CYGB
b
α-SMA
c
merge
F2
d
CYGB
p
e
α-SMA
p
f
merge
p
F3
g
CYGB
p
h
α-SMA
p
i
merge
p
F4
j
CYGB
p
k
α-SMA
p
l
merge
p
F3
m
CYGB
p
n
Thy-1
p
o
merge
p
F3
p
CYGB
p
q
FBLN2
p
r
merge
p

Histoglobin, CYGB, and stellate cell activation-associated protein were classified as human, mouse, and rat homologs of a hexacoordinate globin that differs from the traditional pentacoordinate globins such as myoglobin and hemoglobin.[1–4] CYGB is induced during the activation of rat hepatic stellate cells, which become myofibroblast-like cells, and its expression is increased in fibrotic livers in rodent models.[1] However, it is unclear whether CYGB is expressed in both stellate cells and portal myofibroblasts. Previously, Ogawa *et al*[21] isolated vitamin A-free cells from the nonparenchymal cell fraction in rat livers using FACS analysis. Ogawa *et al*[21] then demonstrated that vitamin A-positive cells are desmin, CYGB, and α-SMA positive and also highly express oxidized low-density lipoprotein receptor 1, endothelin receptor B, and cardiac troponin T. In contrast, vitamin A-free cells are negative for desmin and CYGB but positive for α-SMA and FBLN2. These cell types express high levels of arginine vasopressin receptor V1a (Avpr1a), gremlin, osteopontin, collagen a3(V), and lumican. Thus, Ogawa *et al*[21] concluded that CYGB could be a promising molecular marker of rat hepatic stellate cells. Furthermore, Bosselut *et al*[29] performed a comparative proteomic study to identify markers and gain insight into the distinct functions of myofibroblasts derived from either hepatic stellate cells or portal mesenchymal cells in rats.[21] The two cell types were subjected to comparative analyses by 2-D MS/MS. CYGB was confirmed to have the highest level of overexpression in activated stellate cells, as confirmed by reverse-transcription quantitative real-time PCR, immunoblot, and immunocytochemical analyses. Thus, CYGB was identified as the best marker for distinguishing stellate cells from portal myofibroblasts. The results also suggested different functions for the two cell populations in the liver wound-healing response, with a prominent role for portal myofibroblasts in scar formation. It should be noted that these previous studies confirmed the expression of CYGB in rodent hepatic stellate cells and *in vivo* models, whereas the present study addressed the actual localization of CYGB in human stellate cells, but not in portal myofibroblasts that are positive for FBLN2 and Thy-1.

Definition of Hepatic Myofibroblasts

The term 'myofibroblast' was first proposed by Gabbiani *et al*[30] in 1972 to refer to fibroblastic cells located within granulation tissue that exhibit substantial cytoplasmic microfilaments composed of actin, myosin, and associated proteins.[29] In particular, the microfilaments of myofibroblasts contain α-SMA that is the actin isoform typical of smooth muscle cells located in the vessel wall[30] and has become the most reliable marker for myofibroblastic cells.[31,32] Myofibroblasts are additionally positive for Thy-1.[12,13]

In the liver, hepatic stellate cells and portal fibroblasts are able to acquire a myofibroblastic phenotype,[8,33] although it has remained difficult to distinguish myofibroblastic (activated) stellate cells from portal myofibroblasts in human liver tissue. In the current study, we showed that cells that are positive for both CYGB and CRBP-1 represent the quiescent phenotype of human stellate cells that are uniquely localized in the perisinusoidal space, and cells that are additionally positive for α-SMA are myofibroblastic (activated) human stellate cells that are predominantly present near the fibrotic septum of advanced fibrotic liver tissues. Furthermore, we observed that cells positive for Thy-1 and FBLN2 in normal liver tissues (ie, portal myofibroblasts) were present but scarce around the portal vein area.

Dudas *et al*[12] first reported that Thy-1 is an *in vivo* and *in vitro* marker of rat hepatic myofibroblasts, and later confirmed that Thy-1 is not present in normal or capillarized sinusoids or in isolated rat stellate cells, and that it is neither inducible in isolated stellate cells nor upregulated in myofibroblasts.[14] In accordance with this report, we detected Thy-1 positivity to a limited extent around the portal vein area in the intact human liver and in the extended fibrotic septum of the fibrotic human liver, where portal myofibroblasts are located. Culture experiments using mouse stellate cells confirmed that these cells express CYGB throughout the culture period until day 7 and α-SMA at days 4 and 7, whereas Thy-1 is not expressed throughout this period. Thus, our data also support the hypothesis that Thy-1 is not a marker of hepatic stellate cells in humans or mice, although it is expressed in myofibroblasts around the portal vein area. The reason for the minimal expression of Thy-1 in portal myofibroblasts is not known, although Thy-1 regulates fibroblast focal adhesions, cytoskeletal organization, and cell migration.[34]

FBLN2 is an extracellular matrix protein of the fibulin family that binds various extracellular ligands and calcium. FBLN2 is present in the basement membrane and stroma of several tissues and may play a role in organ development, particularly during the differentiation of heart, skeletal, and neuronal structures. Knittel *et al*[15] reported that FBLN2-positive MFs are detectable in the portal field, vessel walls, and hepatic parenchyma of the normal liver, and their number is increased in the septal regions during liver fibrogenesis in rat models. These findings are similar to

Figure 6 *Double immunofluorescence staining.* CYGB (red in panels **a**, **d**, **g**, and **j**; green in panels **m** and **p**), α-SMA (green in panels **b**, **e**, **h**, and **k**), DAPI (blue), Thy-1 (red in panel **n**), and FBLN2 (red in panel **q**) are shown. Merged photographs of CYGB and α-SMA, FBLN2, or Thy-1 are also presented. CYGB was expressed in the parenchyma and inside hepatocytic nodules. Cells constituting the fibrotic septum in advanced fibrosis (F3) were positive for α-SMA but negative for CYGB. CYGB and α-SMA double-positive cells were occasionally present around the fibrotic septum of F4 liver (**i**). CYGB-positive cells did not overlap with cells that were positive for Thy-1 or FBLN2 (**o** and **r**). Bar, 100 μm.

our present observations in diseased human livers. Thus, FBLN2 and Thy-1 are reliable cellular markers of portal myofibroblasts that differ from stellate cells that are positive for CYGB and CRBP-1 in intact and fibrotic human livers. In the portal area, MFs that are negative for CYGB are the main cells that induce fibrotic septum formation. Thus, targeting of these cells in addition to stellate cells has therapeutic potential for controlling fibrotic septum development.

Cellular Markers of Hepatic Stellate Cells

Based on our present results, we emphasize the superiority of CYGB as a marker of human stellate cells in both intact and fibrotic livers. Several markers of stellate cells have been reported in rodents and humans. Stellate cells store vitamin A-containing lipid droplets, suggesting that vitamin A may be a useful marker of stellate cells.[35] However, a specific staining method to identify vitamin A or related compounds,

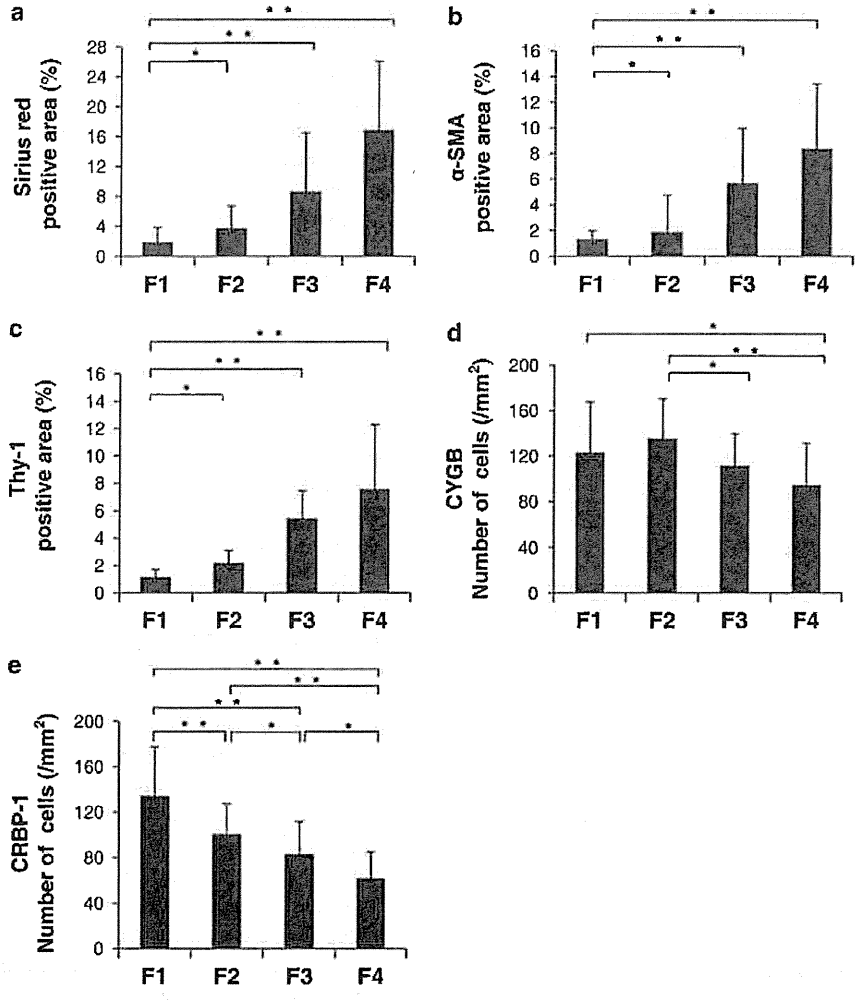

Figure 7 Morphometric analysis. (**a**–**c**) Correlation between hepatic fibrosis stage (according to the new Inuyama classification) and the ratio of the Sirius red-positive area (**a**), α-SMA-positive area, (**b**) or Thy-1-positive area (**c**). Positive areas for Sirius red, α-SMA, or Thy-1 immunohistochemistry were determined using Lumina Vision 2.4 bio-imaging software (Mitani Corporation, Tokyo, Japan). Note that the Sirius red-positive area, α-SMA-positive area, and Thy-1-positive area increased with the progression of liver fibrosis. (**d**, **e**) CYGB or CRBP-1-positive cells were counted in a 1.4 mm^2 area under a × 100 objective. Note that the CYGB- and CRBP-1-positive cell numbers decreased as liver fibrosis progressed. $^*P<0.05$, $^{**}P<0.01$.

Figure 8 CYGB expression in primary cultured mouse stellate cells. After 1 day of culture following isolation, mouse HSCs adhered to plastic plates and exhibited round cell bodies with numerous lipid droplets similar to those observed in lipocytes. Cell bodies then began to gradually spread and flatten, increasing in size and losing lipid droplets, resulting in the activated myofibroblastic phenotype. (**a**) Immunocytochemical analyses confirmed the expression of CYGB throughout the experimental period (A–C), and α-SMA was detected at days 4 and 7 (D–F). Double immunofluorescence showed that activated mouse stellate cells were positive for both Cygb and α-SMA (G, H, I). Under identical culture conditions, Thy-1 was not observed in mouse stellate cells (M, N, O) that were positive for Cygb (J–L, P–R). Bar, 20 μm. (**b**) Immunoblot analyses confirmed the presence of CYGB at days 1, 4, and 7 and α-SMA at days 4 and 7. Thy-1 was not detected throughout the culture period.

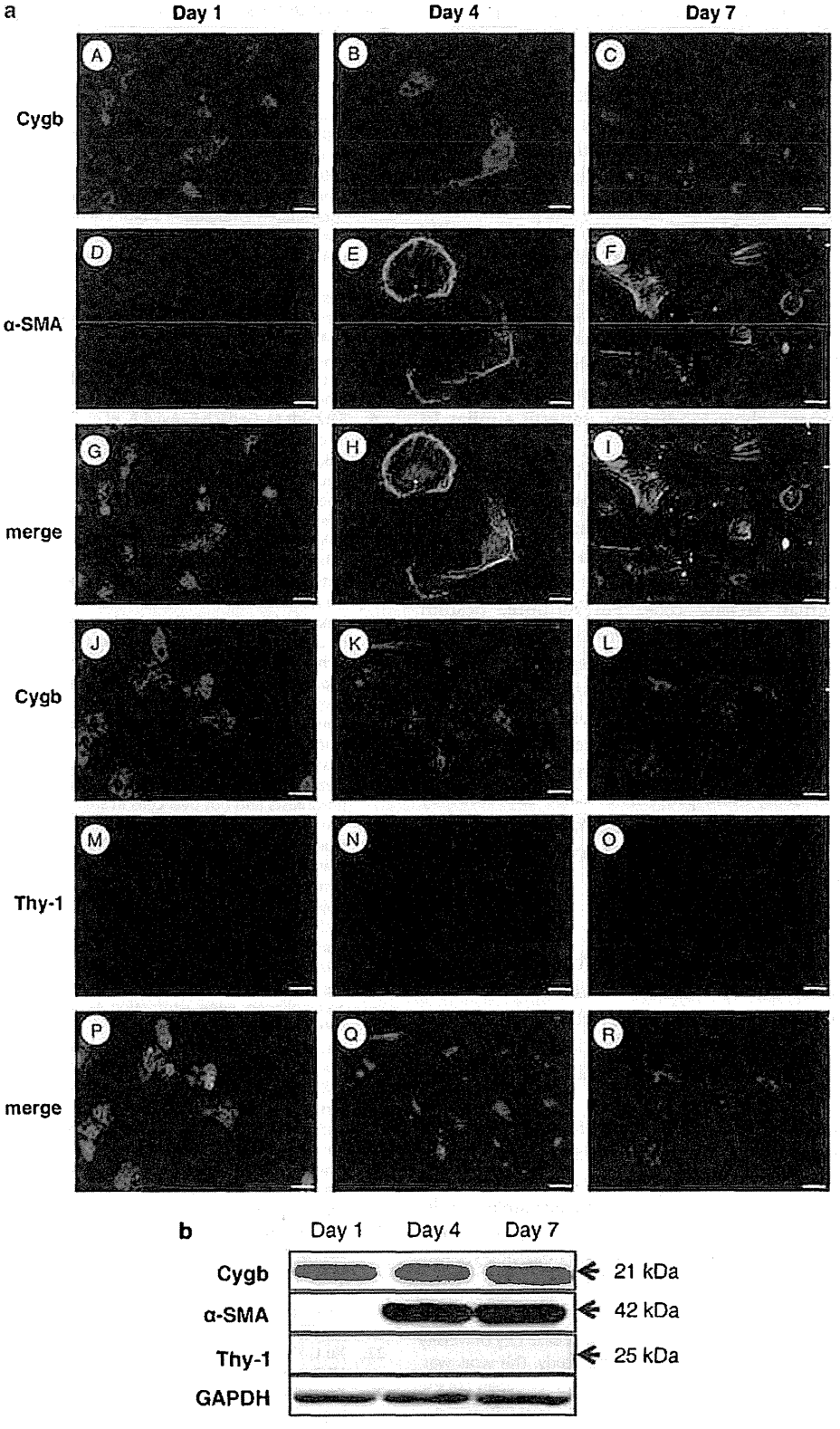
a
Day 1
Day 4
Day 7
Cygb
α-SMA
merge
Cygb
Thy-1
merge
A
B
C
D
E
F
G
H
I
J
K
L
M
N
O
P
Q
R
b
Day 1
Day 4
Day 7
Cygb
α-SMA
Thy-1
GAPDH
21 kDa
42 kDa
25 kDa

such as retinol and retinoic acid, has not been developed, and detection of these compounds via fluorescence microscopy is inconvenient for fixed human liver tissues obtained via clinical procedures. In this context, the use of CRBP-1, a carrier protein of intracellular retinol, is reasonable.[11] CRBP-1 was observed to be downregulated in human livers with advanced fibrosis (Figure 7), presumably because of the loss of vitamin A in stellate cells upon cell activation.

As discussed above, α-SMA is frequently used as a marker of activated and myofibroblastic stellate cells.[29–33] However, this cytoskeletal protein is also expressed in portal myofibroblasts and vascular smooth muscle cells in the arteries, portal vein, and central veins, indicating that α-SMA is not specific for stellate cells. Vinculin, a membrane-cytoskeletal protein in focal adhesion plaques, and synemin, an intermediate filament, show localization patterns similar to that of α-SMA.[36,37]

Desmin, a 52 kD protein that is a subunit of intermediate filaments in skeletal muscle, smooth muscle, and cardiac muscle, was originally identified as a stellate cell marker by Yokoi *et al*[10] in 1984. Desmin is clearly detectable in mouse and rat stellate cells in tissue and in primary culture but not expressed by human stellate cells. Furthermore, desmin expression in rodent hepatic stellate cells has been reported to be both heterogeneous and location dependent.[38] Thus, desmin is no longer considered to be a specific marker of stellate cells. Although neural cell adhesion molecule (also known as CD56) and the intermediate proteins glial fibrillary acidic protein and vimentin have frequently been used as markers of stellate cells, these proteins are also expressed by myofibroblasts.[39,40] In addition, although neurotrophin-3 is specific for stellate cells, it disappears in activated stellate cells in human tissue.[41]

CONCLUSIONS

Taken together, our findings reveal that CYGB is an excellent marker for quiescent and activated stellate cells in both intact and fibrotic human liver. Because the identity of the cell types that participate in collagen production and the fibrotic process in the diseased human liver (caused by hepatitis B or C virus infection, alcohol abuse, obesity, or autoimmune disease) is controversial and because myofibroblasts can be derived from stellate cells, portal myofibroblasts, mesothelial cells,[42] and the epithelial–mesenchymal transition,[43] a molecular marker that is able to uniquely trace stellate cells inhuman liver tissues will be valuable for studying the pathogenesis and fibrotic process of human liver disease.

ACKNOWLEDGMENTS

We thank Professor Kazuo Ikeda and Dr Keiko Iwaisako, Osaka City University Medical School, for their valuable comments on this study. This work was supported by a Grant-in-Aid for Scientific Research from the Japan Society for the Promotion of Science (JSPS) (no. 21390232; 2009–2011; to NK); a grant from the Ministry of Health, Labour, and Welfare of Japan (2008–2010; to NK); and a Thrust Area Research Grant from Osaka City University (2008–2012; to NK).

DISCLOSURE/CONFLICT OF INTEREST

The authors declare no conflict of interest.

1. Kawada N, Kristensen DB, Asahina K, *et al.* Characterization of a stellate cell activation-associated protein (STAP) with peroxidase activity found in rat hepatic stellate cells. J Biol Chem 2001;276:25318–25323.
2. Trent 3rd JT, Hargrove MS. A ubiquitously expressed human hexacoordinate hemoglobin. J Biol Chem 2002;277:19538–19545.
3. Burmester T, Ebner B, Weich B, *et al.* Cytoglobin: a novel globin type ubiquitously expressed in vertebrate tissues. Mol Biol Evol 2002;19:416–421.
4. Pesce A, Bolognesi M, Bocedi A, *et al.* Neuroglobin and cytoglobin. Fresh blood for the vertebrate globin family. EMBO Rep 2002;3:1146–1151.
5. Sawai H, Kawada N, Yoshizato K, *et al.* Characterization of the heme environmental structure of cytoglobin, a fourth globin in humans. Biochemistry 2003;42:5133–5142.
6. Schmidt M, Gerlach F, Avivi A, *et al.* Cytoglobin is a respiratory protein in connective tissue and neurons, which is up-regulated by hypoxia. J Biol Chem 2004;279:8063–8069.
7. Geuens E, Brouns I, Flamez D, *et al.* A globin in the nucleus! J Biol Chem 2003;278:30417–30420.
8. Friedman SL. Hepatic stellate cells: protean, multifunctional, and enigmatic cells of the liver. Physiol Rev. 2008;88:125–172.
9. Scholten D, Osterreicher CH, Scholten A, *et al.* Genetic labeling does not detect epithelial-to-mesenchymal transition of cholangiocytes in liver fibrosis in mice. Gastroenterology 2010;139:987–998.
10. Yokoi Y, Namihisa T, Kuroda H, *et al.* Immunocytochemical detection of desmin in fat-storing cells (Ito cells). Hepatology 1984;4:709–714.
11. Uchio K, Tuchweber B, Manabe N, *et al.* Cellular retinol-binding protein-1 expression and modulation during in vivo and in vitro myofibroblastic differentiation of rat hepatic stellate cells and portal fibroblasts. Lab Invest 2002;82:619–628.
12. Dudas J, Mansuroglu T, Batusic D, *et al.* Thy-1 is an in vivo and in vitro marker of liver myofibroblasts. Cell Tissue Res 2007;329:503–514.
13. Dezso K, Jelnes P, László V, *et al.* Thy-1 is expressed in hepatic myofibroblasts and not oval cells in stem cell-mediated liver regeneration. Am J Pathol 2007;171:1529–1537.
14. Dudas J, Mansuroglu T, Batusic D, *et al.* Thy-1 is expressed in myofibroblasts but not found in hepatic stellate cells following liver injury. Histochem Cell Biol 2009;131:115–127.
15. Knittel T, Kobold D, Saile B, *et al.* Rat liver myofibroblasts and hepatic stellate cells: different cell populations of the fibroblast lineage with fibrogenic potential. Gastroenterology 1999;117:1205–1221.
16. Uyama N, Iimuro Y, Kawada N, *et al.* Fascin, a novel marker of human hepatic stellate cells, may regulate their proliferation, migration, and collagen gene expression through the FAK-PI3K-Akt pathway. Lab Invest 2012;92:57–71.
17. Piscaglia F, Dudás J, Knittel T, *et al.* Expression of ECM proteins fibulin-1 and -2 in acute and chronic liver disease and in cultured rat liver cells. Cell Tissue Res 2009;337:449–462.
18. Janiec DJ, Jacobson ER, Freeth A, *et al.* Histologic variation of grade and stage of non-alcoholic fatty liver disease in liver biopsies. Obes Surg 2005;15:497–501.
19. Ichida F, Tsuji T, Omata M, *et al.* New Inuyama classification; new criteria for histological assessment of chronic hepatitis. Int Hepatol Com 1996;6:112–119.
20. Mori M, Fujii H, Ogawa T, *et al.* Close correlation of liver stiffness with collagen deposition and presence of myofibroblasts in non-alcoholic fatty liver disease. Hepatol Res 2011;41:897–903.
21. Ogawa T, Tateno C, Asahina K, *et al.* Identification of vitamin A-free cells in a stellate cell-enriched fraction of normal rat liver as myofibroblasts. Histochem Cell Biol 2007;127:161–174.
22. Xu L, Hui AY, Albanis E, *et al.* Human hepatic stellate cell lines, LX-1 and LX-2: new tools for analysis of hepatic fibrosis. Gut 2005;54:142–151.
23. Kristensen DB, Kawada N, Imamura K, *et al.* Proteome analysis of rat hepatic stellate cells. Hepatology 2000;32:268–277.
24. Mu YP, Ogawa T, Kawada N. Reversibility of fibrosis, inflammation, and endoplasmic reticulum stress in the liver of rats fed a methionine-choline-deficient diet. Lab Invest 2010;90:245–256.

25. Nakatani K, Okuyama H, Shimahara Y, *et al.* Cytoglobin/STAP, its unique localization in splanchnic fibroblast-like cells and function in organ fibrogenesis. Lab Invest 2004;84:91–101.
26. Sugimoto H, Makino M, Sawai H, *et al.* Structural basis of human cytoglobin for ligand binding. J Mol Biol 2004;339:873–885.
27. Mathew J, Hines JE, Toole K, *et al.* Quantitative analysis of macrophages and perisinusoidal cells in primary biliary cirrhosis. Histopathology 1994;25:65–70.
28. Mouta Carreira C, Nasser SM, di Tomaso E, *et al.* LYVE-1 is not restricted to the lymph vessels: expression in normal liver blood sinusoids and down-regulation in human liver cancer and cirrhosis. Cancer Res 2001;61:8079–8084.
29. Bosselut N, Housset C, Marcelo P, *et al.* Distinct proteomic features of two fibrogenic liver cell populations: hepatic stellate cells and portal myofibroblasts. Proteomics 2010;10:1017–1028.
30. Gabbiani G, Majno G. Dupuytren's contracture: fibroblast contraction? An ultrastructural study. Am J Pathol 1972;66:131–146.
31. Darby I, Skalli O, Gabbiani G. Alpha-smooth muscle actin is transiently expressed by myofibroblasts during experimental wound healing. Lab Invest 1990;63:21–29.
32. Gabbiani G. The myofibroblast in wound healing and fibrocontractive diseases. J Pathol 2003;200:500–503.
33. Desmoulière A, Tuchweber B, Gabbiani G. Role of the myofibroblast differentiation during liver fibrosis. J Hepatol 1995;22(2 Suppl):61–64.
34. Niki T, Rombouts K, De Bleser P, *et al.* A histone deacetylase inhibitor, trichostatin A, suppresses myofibroblastic differentiation of rat hepatic stellate cells in primary culture. Hepatology 1999;29:858–867.
35. Wake K. Perisinusoidal stellate cells (fat-storing cells, interstitial cells, lipocytes), their related structure in and around the liver sinusoids, and vitamin A-storing cells in extrahepatic organs. Int Rev Cytol 1980;66:303–353.
36. Rege TA, Hagood JS. Thy-1 as a regulator of cell-cell and cell-matrix interactions in axon regeneration, apoptosis, adhesion, migration, cancer, and fibrosis. FASEB J 2006;20:1045–1054.
37. Kawai S, Enzan H, Hayashi Y, *et al.* Vinculin: a novel marker for quiescent and activated hepatic stellate cells in human and rat livers. Virchows Arch 2003;443:78–86.
38. Uyama N, Zhao L, Van Rossen E, *et al.* Hepatic stellate cells express synemin, a protein bridging intermediate filaments to focal adhesions. Gut 2006;55:1276–1289.
39. Wake K, Sato T. Intralobular heterogeneity of perisinusoidal stellate cells in porcine liver. Cell Tissue Res 1993;273:227–237.
40. Nakatani K, Seki S, Kawada N, *et al.* Expression of neural cell adhesion molecule (N-CAM) in perisinusoidal stellate cells of the human liver. Cell Tissue Res 1996;283:159–165.
41. Cassiman D, Libbrecht L, Desmet V, *et al.* Hepatic stellate cell/myofibroblast subpopulations in fibrotic human and rat livers. J Hepatol 2002;36:200–209.
42. Cassiman D, Denef C, Desmet VJ, *et al.* Human and rat hepatic stellate cells express neurotrophins and neurotrophin receptors. Hepatology 2001;33:148–158.
43. Li Y, Wang J, Asahina K. Mesothelial cells give rise to hepatic stellate cells and myofibroblasts via mesothelial-mesenchymal transition in liver injury. Proc Natl Acad Sci USA 2013;110:2324–2329.

Title

Efficient engraftment of human iPS cell-derived hepatocyte-like cells in uPA/SCID mice by overexpression of *FNK*, a Bcl-x_L mutant gene

Running head: Efficient engraftment of human iPS-HLCs

Yasuhito Nagamoto[1,2], Kazuo Takayama[1,2,3], Katsuhisa Tashiro[4], Chise Tateno[5], Fuminori Sakurai[1], Masashi Tachibana[1], Kenji Kawabata[4], Kazuo Ikeda[6], Yasuhito Tanaka[7], & Hiroyuki Mizuguchi[1,2,3,8*]

1 Laboratory of Biochemistry and Molecular Biology, Graduate School of Pharmaceutical Sciences, Osaka University, Osaka 565-0871, Japan; 2 Laboratory of Hepatocyte Regulation, National Institute of Biomedical Innovation, Osaka 567-0085, Japan; 3 iPS Cell-based Research Project on Hepatic Toxicity and Metabolism, Graduate School of Pharmaceutical Sciences, Osaka University, Osaka567-0871, Japan; 4 Laboratory of Stem Cell Regulation, National Institute of Biomedical Innovation, Osaka 567-0085, Japan; 5 PhoenixBio Co. Ltd., Hiroshima, Japan 739-0046, Japan; 6 Department of Anatomy and Regenerative Biology, Graduate School of Medicine, Osaka City University, Osaka, 545-8585, Japan; 7 Department of Virology and Liver Unit, Graduate School of Medical Sciences, Nagoya City University, Nagoya, 467-8601, Japan; and 8 The Center for Advanced Medical Engineering and Informatics, Osaka University, Osaka 565-0871, Japan.

Correspondence: Dr. Hiroyuki Mizuguchi
Laboratory of Biochemistry and Molecular Biology, Graduate School of Pharmaceutical Sciences, Osaka University, 1-6 Yamadaoka, Suita, Osaka 565-0871, Japan.
Phone: +81-6-6879-8185
FAX: +81-6-6879-8186
E-mail: mizuguch@phs.osaka-u.ac.jp

Key words: iPS cells, hepatocyte, Bcl-x_L, FNK, transplantation

For Review Only

Abstract

Human liver chimeric mice are expected to be applied for drug-toxicity tests and human hepatitis virus research. Human induced pluripotent stem cell-derived hepatocyte-like cells (iPS-HLCs) are a highly attractive donor source for the generation of human liver chimeric mice because they ~~can~~ can be produced on a large scale and established from an individual. Although these cells have been successfully used to generate human liver chimeric mice, there is still room for improvement in the repopulation efficiency. To enhance the repopulation efficacy, the human iPS-HLCs were transduced with an adenovirus vector (Ad-FNK) expressing *FNK*, a hyperactive mutant gene from *Bcl-x_L*, which was expected to inhibit apoptosis in the process of integration into liver parenchyma. We then transplanted Ad-FNK-transduced human iPS-HLCs into urokinase-type plasminogen activator-transgenic severe combined immunodeficiency (uPA/SCID) mice (FNK-mice) and evaluated the repopulation efficacy. The anti-apoptotic effects of the human iPS-HLCs were enhanced by FNK over-expression *in vitro*. Human albumin levels in the transplanted mice were significantly increased by transplantation of Ad-FNK-transduced human iPS-HLCs (about 24,000 ng/ml). Immunohistochemical analysis with an anti-human αAT antibody revealed greater repopulation efficacy in the livers of FNK-mice than control mice. Interestingly, the expression levels of human hepatocyte-related genes in the human iPS-HLCs of FNK-mice were much higher than those in the human iPS-HLCs before transplantation. We succeeded in improving the repopulation efficacy of human liver chimeric mice generated by transplanting the Ad-FNK-transduced human iPS-HLCs into uPA/SCID mice. Our method using ectopic expression of FNK was useful for generating human chimeric mice with high chimerism.

Introduction

Human liver chimeric mice are expected as potent tools for drug-toxicity tests and hepatitis virus research. Several groups have recently reported the generation of human liver chimeric mice by transplantation human hepatocyte-like cells (HLCs) (16,36), which were differentiated from human pluripotent stem cells (including human embryonic stem (ES) cells (34) and induced pluripotent stem (iPS) cells (26)). However, to the best our knowledge, the highest concentration of human albumin (ALB) in blood of human liver chimeric mice with human ES/iPS cell-derived HLCs (ES/iPS-HLCs) in previous reports was approximately 4,000 ng/ml (37). The repopulation efficacy of these mice is not sufficient for their applications. Therefore, the chimerism of human liver chimeric mice with human ES/iPS-HLCs will need to be enhanced before these mice can be used in medical applications.

In general, the repopulation efficacy of human ES/iPS-HLCs in human liver chimeric mice depends on many factors, such as the types of immunodeficient mice with liver injury and characteristics of donor cells. With regard to the recipient mice, high-severity of immunodeficiency and liver injury of them facilitate to replace mice hepatocytes with cryopreserved human hepatocytes (8,24). Previously, several mouse models for the generation of human liver chimeric mice were developed to meet the requirements described above (i.e., urokinase-type plasminogen activator-transgenic severe combined immunodeficiency (uPA/SCID) mice (33), fumarylacetoacetate hydrolase and recombination activating gene 2 and interleukin 2 receptor gamma chain deficient ($Fah^{-/-}Rag2^{-/-}IL2rg^{-/-}$) mice (3), and herpes simplex virus type 1 thymidine kinase-transgenic NOG (TK-NOG) mice (7)). Among these mouse models, uPA/SCID mice are widely used to generate human liver chimeric mice with almost completely humanized livers and human liver functions through the transplantation of cryopreserved human hepatocytes (9,23,33). With regard to donor cells, human iPS-HLCs whose characteristics are equivalent to those of cryopreserved human hepatocytes might be required for highly repopulated human liver chimeric mice. It is thus important to promote the hepatic maturation of human iPS-HLCs. We have recently succeeded in generating highly functional human iPS-HLCs by a combination of over-expression of hepatic transcription factors and three-dimensional (3D) culture (21,27,28,30). The expression levels of various hepatocyte-related genes were comparable between human iPS-HLCs and primary human hepatocytes (30). These matured human iPS-HLCs might be appropriate as donor cells to generate human liver chimeric mice with high chimerism.

It is known that a large fraction of transplanted hepatocytes rapidly undergo apoptotic death and is removed from the recipient liver through phagocytosis by macrophages (6). Thus, it might be reasonable to presume that the engraftment efficacy would be enhanced by regulating the cell survival signals and improving the resistance to apoptotic cell death through over-expression of an anti-apoptotic gene, such as Bcl-x_L. Among the Bcl-2 family proteins synthesized in the normal liver, only the Bcl-x_L and Mcl-1 proteins were detectable at the constitutive basal level (35). In addition, only Bcl-x_L expression was up-regulated in the regenerated liver (35). It has also been reported that hepatocyte-specific Bcl-x_L deficient mice showed spontaneous cell death in hepatocytes (31). In contrast, Bcl-x_L transgenic mice showed resistance against cell death induced using anti-Fas antibody (4,17). These reports suggest that Bcl-x_L may play an important role in the survival of hepatocytes.

In this study, we first examined whether over-expression of FNK (a hyperactive mutant of Bcl-x_L), which is a more powerful artificial anti-apoptotic factor than Bcl-x_L (1), is useful to avoid the induction of apoptosis in an *in vitro* culture model. Next, we attempted to generate human liver chimeric mice by transplanting the FNK-expressing adenovirus (Ad-FNK) vector-transduced human iPS-HLCs, which were differentiated under the 3D culture condition, into uPA/SCID mice. The treatment of the human iPS-HLCs with Ad-FNK successfully increased the concentration of human ALB in mouse blood as well as the repopulation efficacy. The transduction of FNK should be useful for the generation of human liver chimeric mice with iPS-HLCs.

MATERIALS AND METHODS

~~human~~ Human iPS cell culture

A human iPS cell line generated from the human male embryonic lung fibroblast cell line MCR5 was provided from the JCRB Cell Bank (Dotcom, JCRB Number: JCRB1327). This human iPS cell line was maintained on a feeder layer of mitomycin C-treated mouse embryonic fibroblasts (Millipore; PMEF-H) with ReproStem (ReproCELL) supplemented with 10 ng/ml fibroblast growth factor 2 (FGF2, Sigma). Human iPS cells were dissociated with 0.1 mg/ml dispase (Roche Diagnostics) into small clumps and were then subcultured every 5 or 6 days.

Ad vectors

Ad vectors were constructed by an improved *in vitro* ligation method (18,19). We have constructed pHMEF5 (11), which contains the human elongation factor-1a (EF-1a) promoter, and pAdHM41 K7 (12) in previous reports. The FNK gene (1) (kindly provided by Shigeo Ohta, Nippon Medical School) was inserted into pHMEF5 resulting in pHMEF-FNK. The pHMEF-FNK was digested with I-*Ceu*I/PI-*Sce*I (NEB) and ligated into I-*Ceu*I/PI-*Sce*I-digested pAdHM41-K7, resulting in pAd-FNK. The human EF-1a promoter-driven LacZ-, FOXA2-, or HNF1a-expressing Ad vectors (Ad-LacZ, Ad-FOXA2, or Ad-HNF1a, respectively) were constructed previously (28,32). All of Ad vectors contain a stretch of lysine residue (K7) peptides in the C-terminal region of the fiber knob for more efficient transduction of human iPS cells and definitive endodermal cells, in which transfection efficiency was almost 100% (10,27,29), and purified as described previously (20). The vector particle (VP) titer was determined by using a spectrophotometric method (15). We have confirmed that these Ad vector-mediated gene expression continued for 5 days and was almost disappeared at 9 days after transduction by *in vitro* analysis (27). Therefore, Ad vector-mediated FNK expression in the human iPS-HLCs, which were transplanted into uPA/SCID mice, might be disappeared at about 9 days after transplantation.

In vitro differentiation

The hepatic differentiation protocol was based on our previous report (30). On day 34, the human iPS cell-derived cells were transduced with 3000 VP/cell of FNK- or LacZ-expressing Ad vector (Ad-FNK or Ad-LacZ).

Flow cytometry

The human iPS cells were differentiated into HLCs as described in **Figure 1A**. Single-cell suspensions of human iPS cell-derived cells were fixed with 2% paraformaldehyde (PFA; Wako) at 4 °C for 20 min, and then incubated with the anti-asialoglycoprotein receptor 1 (ASGR1) goat antibody (Santa Cruz Biotechnology) followed by the anti-goat IgG antibody labeled with Alexa Fluor 488 (Molecular Probes). Flow cytometry analysis was performed using a FACS LSR Fortessa flow cytometer (BD Biosciences).

Cell viability tests

The human iPS cells were differentiated into HLCs. Cell viability was assessed by using an Alamar Blue assay kit (Biosource). The supernatants of the cells were measured at a wavelength of 570 nm with background subtraction at 600 nm in a plate reader.

Apoptosis inhibiting activity

The human HLCs were cultured in hepatocyte culture medium (HCM, Lonza) supplemented with 20 ng/ml oncostatin M (R&D Systems), 10^{-6} M dexamethasone (Sigma), and apoptotic inducible drug (40 nM Staurosporine or 2 μM A23187 (both from Merck Millipore)) for 4 days. These cells were harvested by using Cell Recovery Solution (BD Biosciences), and ~~T~~the surviving cells were counted by the trypan blue (nacalai tesque) exclusion every day.

Transplantation of the hepatocyte-like cells

The male and female uPA+/+/SCID (uPA/SCID) mice (33) at 2 to 4 weeks after birth were used as the recipient mice. These mice were anesthetized with isoflurane (Pfizer) and injected with the 1 x 10^6 viable human iPS-HLCs through a small left-flank incision into the inferior splenic pole. Hepatocyte Culture Medium (Lonza) was used as injection vehicle. The lower reaches of the injection site were tied with string. After the injection of the cells, the mouse spleens were excised and the superior splenic poles were tied with string. All experiments were conducted in accordance with the ethical approval of PhoenixBio Co., Ltd.

ELISA

The human iPS cells were differentiated into HLCs as described in **Figure 1A**. The culture supernatants, which were incubated for 24 hr after fresh medium was added, were collected. Mice blood samples were collected periodically from the tail vein.

These samples were analyzed for the level of human ALB by ELISA. ELISA kits for human ALB were purchased from Bethyl Laboratolies. ELISA was performed according to the manufacturer's instructions. The ALB secretion levels were calculated according to each standard.

RNA isolation and reverse transcription-polymerase chain reaction (RT-PCR)

Cells or whole mouse livers were homogenized in ISOGENE (Nippon Gene), and then, ~~Total~~ total RNA was isolated ~~using ISOGENE (Nippon Gene)~~ according to the manufacturer's instructions. cDNA was synthesized using 500 ng of total RNA with a Superscript VILO cDNA synthesis kit (Invitrogen). Real-time RT-PCR was performed with Taqman gene expression assays or Fast SYBR Green Master Mix using an ABI Step One Plus (all from Applied Biosystems). Relative quantification was performed against a standard curve and the values were normalized against the input determined for the housekeeping gene, *glyceraldehyde 3-phosphate dehydrogenase* (*GAPDH*). Note that the human *ALB*, *HNF4α*, *αAT*, and *CYP3A4* expression values normalized by the other housekeeping genes, *phosphoglycerate kinase 1* (*PGK1*), *HBS1-like* (*HBS1L*), *succinate dehydrogenase complex subunit A flavoprotein* (*SDHA*), or *transferrin receptor* (*TFRC*), were comparable with the gene expression values normalized by *GAPDH* (data not shown). The human specific primer sequences and assay IDs used in this study are described in **Table 1** and **2**. The human *CYP3A4* primer for Fast SYBR Green Master Mix was used to analyze the gene expression level in the human iPS-HLCs *in vitro*, and the human *CYP3A4* Taqman gene expression assays was used to analyze the gene expression level in the human iPS-HLCs, which was integrated into mice liver. The other human specific primers were also designed to detect only human genes, but not mouse genes.

Immunohistochemistry

Immunohistochemistry of human ALB and human CK8/18 (MP Biomedicals) was performed at PhenixBio (hiroshima). These ~~analysis~~ analyses were used anti-human ALB goat antibody (Bethyl Laboratolies) and anti-human CK8/18 mouse antibody (MP Biomedicals). Immunohistochemistry of human αAT was performed as follows. Recipient mouse livers were harvested at 4 weeks after human cell transplantation. The livers were fixed with 10% neutral buffered formalin (Wako), embedded in paraffin and sectioned at 5 μm. Pretreatment of the paraffin tissue sections consisted of L.A.B. Solution (Polysciences, Inc.) at room temperature for 15 min. After incubation with 0.1% Tween 20 (Sigma) and blocking with ImmunoBlock

(DS ParmaBioMedical), the sections were incubated with an anti-human αAT rabbit antibody (Dako; 1:50) at 4 °C overnight, followed by incubation with an anti-rabbit IgG biotinylated-antibody (Vector Lab.; 1:100) at room temperature for 1 hr. Immunoreactivities for human αAT were visualized with a VECTASTAIN ABC kit and ImmPACT DAB Substrate (all from Vector Lab.) according to the manufacturer's instructions. The sections were counterstained with Mayer's hematoxylin (Wako). The repopulation efficacy was calculated as the ratio of human αAT-expressing areas to the total liver section area using ImageJ. This analysis was performed using the 3 sections from each 2 lobe of mouse liver, that is, we took 6 sections per mouse.

Statistical analysis

All data are represented as means ± SD or SE from at least three independent experiments. Statistical an_alysiswas performed using the unpaired two-tailed Student's *t*-test.

RESULTS

FNK enhanced the resistance of the human iPS-HLCs to apoptotic stimulations.

To generate the human iPS-HLCs, hepatic differentiation was performed using a stage-specific transient transduction of FOXA2 and HNF1α (28), and a 3D culture method (30) as shown in **Figure 1A**. On day 34, the human iPS-HLCs were transduced with Ad-LacZ or Ad-FNK, and then hepatocyte characteristics, such as the gene expression levels of hepatocyte-related markers (**Fig. 1B**), the ability to secrete ALB (**Fig. 1C**), and the percentage of ASGR1 (a mature hepatocyte marker)-positive cells (**Fig. 1D**), were compared in the Ad-LacZ- and Ad-FNK-transduced human iPS-HLCs on the next day. As a result, the hepatic characteristics of the Ad-FNK-transduced human iPS-HLCs were similar to those of the Ad-LacZ-transduced human iPS-HLCs, suggesting that the transient over-expression of FNK did not influence the hepatic characteristics. Moreover, the gene expression levels of *ALB* and *CYP3A4* ~~and the amount of ALB secretion~~ in the human iPS-HLCs were comparable to those in primary human hepatocytes (PHs) that were cultured 48 hr after plating the cells. Thus, these results suggested that efficient hepatic differentiation was successfully achieved. Next, we examined whether FNK over-expression had the ability to enhance the resistance to apoptotic stimulations. The number of viable human iPS-HLCs was measured in the presence of the apoptosis-inducing drugs, Staurosporine (an inhibitor of protein kinase C) and A23187 (a calcium ionophore) (**Fig. 1F** and **Fig. 1G**, respectively). Although the cell viabilities were not affected by the transduction of Ad-FNK (**Fig. 1E**), the number of surviving Ad-FNK-transduced human iPS-HLCs was higher than the number of surviving Ad-LacZ-transduced human iPS-HLCs in the presence of apoptosis-inducing drugs. These results suggests that FNK over-expression in the human iPS-HLCs could enhance the tolerance to apoptotic stimulations without influence on the expression of hepatic markers.

The human ALB concentration was enhanced by the transplantation of Ad-FNK-transduced human iPS-HLCs.

In order to determine whether the engraftment and repopulation efficacy of human iPS-HLCs in immunodeficient mice with damaged livers could be increased by Ad-FNK transduction, we transplanted Ad-LacZ- or Ad-FNK-transduced human iPS-HLCs into uPA/SCID mice by intrasplenic injection (LacZ-mice and FNK-mice, respectively). Because it has been found that some intrasplenic injected hepatocytes engraft into recipient spleen (25), the recipient spleen was excised just after

transplantation of human iPS-HLCs to avoid influences of engrafted human iPS-HLCs in the recipient spleen. The experimental design of the cell transplantation is shown in **Figure 2A**. Because it is known that the human ALB concentration in mouse blood correlates with the number of repopulated human hepatocytes in mice transplanted with cryopreserved human hepatocytes (3,33), we monitored the human ALB concentration in the blood of LacZ- and FNK-mice (**Fig. 2B**). Human ALB in the blood of both LacZ- and FNK-mice was detectable at 1 week after transplantation. The human ALB concentration in the FNK-mice (approximately 73 ng/ml) was slightly higher than that in the LacZ-mice (approximately 30 ng/ml). Thereafter, the human ALB concentration in these two groups was increased until 4 weeks after transplantation (to approximately 7,400 ng/ml in the LacZ-mice, and approximately 24,000 ng/ml in the FNK-mice). The human ALB concentration in the blood of FNK-mice was significantly higher than that in the blood of LacZ-mice at 2-4 weeks after transplantation. Unfortunately, both LacZ- and FNK-mice became weak at 4 weeks after transplantation, and were therefore ~~At 4 weeks after transplantation, the mice were~~ sacrificed at this time point. No distinct tumor was observable at the time of sacrificed.~~, and~~ ~~t~~The gene expression levels of hepatocyte-specific markers in the human iPS-HLCs in the LacZ- or FNK-mice were measured by using human specific primers. First, the expression level of human *ALB* in the human iPS-HLCs was analyzed by real-time RT-PCR (**Fig. 2C**). Because there were no significant differences between these two groups, the human ALB secretion ability of the human iPS-HLCs in FNK-mice would be similar to that of the human iPS-HLCs in LacZ-mice. Therefore, the difference in the human ALB concentration between the LacZ-mice and the FNK-mice would ~~have been~~be due to the repopulation efficacy of the human iPS-HLCs, but not due to a difference between the human ALB secretion ability of the human iPS-HLCs in the LacZ-mice and that in the FNK-mice. Taken together, these results suggest that the number of the repopulated human iPS-HLCs in the FNK-mice was higher than that in the LacZ-mice.

The gene expression levels of hepatocyte-related genes in the human iPS-HLCs were up-regulated in the mouse liver.

To examine whether the hepatic functionalities of the human iPS-HLCs were enhanced by transplantation into uPA/SCID mice, the gene expression levels of human hepatocyte-related markers in the human iPS-HLCs that were engrafted ~~recovered from~~into the liver of ~~the~~ FNK-mice, were compared at 4 weeks after transplantation (post-transplant)~~ were compared~~ with those in the human iPS-HLCs ~~which~~ that were not transplanted (pre-transplant) (**Fig. 3**). Interestingly, the gene expression levels of

human *ALB*, human *αAT*, human *ASGR1*, human *HNF4α*, human *CYP3A4*, human *CYP2D6*, human *CYP7A1*, human *CYP3A5*, human *UGT1A1*, human *UGT1A3*, human *FXR*, and human *PXR* were drastically up-regulated after transplantation. These results might suggest that the human iPS-HLCs were maturated in the livers of uPA/SCID mice.

FNK could increase the repopulation efficacy of the human iPS-HLCs in the mouse liver.

To ascertain whether the human iPS-HLCs could repopulate the mouse liver, immunohistochemical analyses were performed by using anti-human-specific antibodies that react with hepatocyte-specific markers. Several clusters of human ALB- (**Fig. 4A**), human αAT- (**Fig. 4B**) and human CK8/18-expressing cells (**Fig. 4C**) were found in the liver sections of FNK-mice. The human hepatocyte-specific marker-positive clusters were also observed in the LacZ-mice (data not shown). These results suggest that the human iPS-HLCs have the potential to repopulate and express human hepatic proteins in the mouse liver. Because some non-specific staining of human ALB-antibody was observed ~~Furthermore~~, we calculated the repopulation efficacy of the human iPS-HLCs in the LacZ or FNK-mice by estimating the ratio of the human αAT-expressing areas to the total liver section area (**Fig. 4D**). The repopulation efficacy of the Ad-FNK-transduced human iPS-HLCs was significantly higher than that of the Ad-LacZ-transduced human iPS-HLCs. Taken together, these results reveal that the transduction of Ad-FNK into human iPS-HLCs would be a useful tool to efficiently repopulate the mouse liver.

DISCUSSION

This study aimed to improve the repopulation efficacy of the human iPS-HLCs in the mice liver for medical applications. To generate chimeric mice with a high level of human liver chimerism, the anti-apoptotic gene (FNK)-transduced human iPS-HLCs were transplanted into uPA/SCID mice. The levels of human ALB and repopulation efficacy in the FNK-mice were higher than those in the LacZ-mice (**Figs. 2** and **4**). On intrasplenic injection in hepatocyte transplantation, a major fraction of transplanted cells (more than 70%) was rapidly removed by phagocyte and macrophage responses (6). The residual transplanted hepatocytes were translocated from the liver sinusoids to the liver plate at between 16 and 20 hr after transplantation. Because transplanted hepatocytes lose intimate contact with the extracellular matrix or other cells during this period, these cells might cause anoikis through the activation of caspase-8 (5,22). It is known that the ectopic expression of Bcl-x_L can inhibit apoptosis by ~~supressing~~suppression of caspase-8, 7, and 3 (14). These facts suggest that the transplanted human iPS-HLCs would be protected from apoptosis in the early period after transplantation by FNK over-expression, and then these cells could translocate from the liver sinusoids to the liver plate of recipient mice.

Although Bcl-x_L is known as a cellular oncogene, no distinct tumors were observed in the FNK-mice at 4 weeks after transplantation. This result suggests that the transient transduction of FNK using Ad vector might not be involve in the tumorigenesis of transplanted human iPS-HLCs. Consistent with this idea, a previous study showed that Ad vector-mediated FNK overexpression did not transform dendritic cells using a colony formation assay in soft agar (38). Taken together, these result indicate that FNK overexpression would be a useful method to enhance the engraftment efficacy of transplanted cells.

The concentration of human ALB in the blood of FNK-mice was significantly higher than that in the blood of LacZ-mice (**Fig. 2A**). In addition, ~~this~~ the concentration in the blood of FNK-mice (about 24,000 ng/ml) was approximately 6-fold higher than that in the blood of mice in the previous study (about 4,000 ng/ml) (37). However, this concentration of human ALB in the blood of FNK-mice, whose repopulation efficacy was about 44~~19~~%, was approximately ~~50~~ 42 times lower than that in the blood of human liver chimeric mice generated by transplantation of cryopreserved human hepatocytes into uPA/SCID mice (about ~~2~~ 1 mg/ml), whose repopulation efficacy was ~~35–50~~about 20% (33). Because the repopulation efficacies were similar in these two groups, it was suggested that the lower ability of the FNK-mice to secrete human ALB into the blood was due to the immaturity of the hepatic functionalities of